



Low temperature XPS of sensitive molecules: Titanium butoxide photoelectron spectra

Mark A. Isaacs^{a,b,*}

^a HarwellXPS, Research Complex at Harwell, Rutherford Appleton Labs, OX16 0FA

^b Department of Chemistry, University College London, 20 Gordon Street, London, WC1H 0AJ

ARTICLE INFO

Keywords:
CryoXPS
Alkoxides
Nanocomposite synthesis
XPS

ABSTRACT

XPS analysis of soft materials remains a challenging task, with sample degradation presenting itself across a wide range of different materials. Correct protocols when performing the experimental spectral acquisition will ensure minimal proliferation of errors in terms of scientific understanding during subsequent data treatments. Furthermore, XPS spectra of titanium butoxide will provide a valuable reference for the materials understanding of alkoxide based metal oxide and mixed-metal oxide functional systems.

1. Introduction

Metal alkoxides are a prominent reagent in the production of metal- and mixed-metal oxides, widely used in numerous fields including catalysis, [1–3] photovoltaics [4,5] and medical materials. [6,7] The ability to undergo facile hydrolysis and condensation enables their application in the synthesis of many metal oxide and mixed metal oxide systems. Metal alkoxides have been crucial reagents in a wide number of intricate and advanced nanocomposites, where spatial locale of grafted sites is critical. [8] Obtaining reference spectra of such compounds will prove a highly valuable resource for advanced materials design of nanocomposites and aid in the spectral deconvolution and understanding of synthesised oxides and mixed oxide materials in which alkoxides are a building block.

They also find notable use as surface modifiers for structurally useful, but chemically inert, high surface area materials such as SBA-15. [8–11] Given their prominence as modifiers of the material-environment interface, materials arising from the use of metal alkoxides are routinely studied by XPS – though reference spectra of the unadulterated precursors are rarely found in literature given the compound propensity to react with moisture to form solid metal oxides. Of additional difficulty is the analysis of those precursors existing in the liquid phase, which are unsuitable for analysis under UHV conditions given the incompatibility between the molecular vapour pressure and the analysis chamber pressure.

Application of cooling processes within an XPS chamber enables analysis of systems which may otherwise be incompatible with vacuum

systems due to unfavourable vapour pressures (e.g. water), [12] or systems which may otherwise degrade under analysis conditions (e.g. due to photon induced degradation). [13] The use of such techniques has thus far primarily been largely favoured for microbiological [12,14–16] or mineral [17–19] science – though it has found use in the analysis of soft materials [20] and even air-sensitive volatile compounds. [21] It is with this application in mind that this work seeks to underline the potential of sample cooling for the understanding of otherwise incompatible materials and molecules.

Low temperature XPS may be used to overcome these challenges, [20–22] by providing an environment by which environmental moisture is removed (thanks to the inherent UHV conditions of standard XPS) but in which the issue of vapour pressure be overcome by the use of cooling techniques.

In this work we look at the analysis of a very commonly used metal alkoxide - titanium butoxide (TBu, Fig. 1) - by low temperature XPS and the experimental handling methods by which appropriate spectra may be obtained. We report photoemission properties for reference, and monitor the sample degradation behaviour upon X-ray exposure.

2. Experimental

Titanium butoxide (CAS: 5593-70-4) was sourced from Sigma-Aldrich (reagent grade, 97%) and was used with no further processing or treatment, deposited directly onto the cooling stage.

CryoXPS data was acquired using a Kratos Axis SUPRA using monochromated Al $K\alpha$ (1486.69 eV) X-rays at 15 mA emission and 12 kV HT

* Corresponding author

E-mail address: mark.isaacs@ucl.ac.uk.

<https://doi.org/10.1016/j.apsadv.2023.100467>

Received 18 July 2023; Received in revised form 3 October 2023; Accepted 3 October 2023

Available online 7 October 2023

2666-5239/© 2023 The Author. Published by Elsevier B.V. This is an open access article under the CC BY-NC-ND license (<http://creativecommons.org/licenses/by-nc-nd/4.0/>).

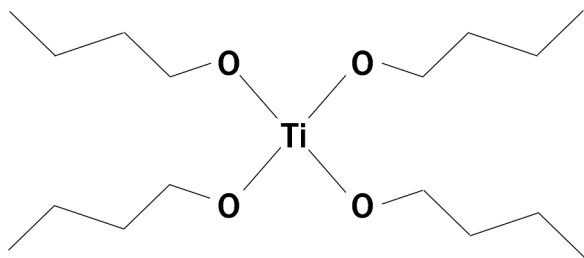


Fig. 1. Titanium butoxide

(180W) unless otherwise stated and a spot size/analysis area of $700 \times 300 \mu\text{m}$. The instrument was calibrated to gold metal Au 4f (83.95 eV) and dispersion adjusted give a BE of 932.6 eV for the Cu 2p_{3/2} line of metallic copper. Ag 3d_{5/2} line FWHM at 10 eV pass energy was 0.5 eV. Source resolution for monochromatic Al K α X-rays is ~ 0.3 eV. The instrumental resolution was determined to be 0.3 eV at 10 eV pass energy using the Fermi edge of the valence band for metallic silver. Resolution with charge compensation system on < 1.33 eV FWHM on PTFE. High resolution spectra were obtained using a pass energy of 20 eV, step size of 0.1 eV and sweep time of 60s, resulting in a line width of 0.7 eV for Au 4f_{7/2}. Survey spectra were obtained using a pass energy of 160 eV. Charge neutralisation was achieved using an electron flood gun with filament current = 0.4 A, charge balance = 2 V, filament bias = 4.2 V. Successful neutralisation was adjudged by analysing the C 1s region wherein a sharp peak with no lower BE structure was obtained. Spectra have been charge corrected to the main line of the carbon 1s spectrum (CC/CH) set to 284.8 eV. All data was recorded at a base pressure of below 9×10^{-9} Torr. Calibration data was recorded at a room temperature of 294 K.

Samples were pre-cooled in the flexi-lock/sample transfer chamber at ambient pressure to -30°C , before being subjected to a roughing

vacuum up to 1×10^{-2} Torr with a concomitant decrease in temperature to -50°C . The pressure was then lowered using turbomolecular pumps to 5×10^{-8} and a temperature of -110°C . The cooling line was then disconnected and the sample transferred to the analysis chamber, at which point the cooling/thermocouple was reconnected. The temperature differential during transfer was $+15^\circ\text{C}$ at its maximum. The sample was allowed to cool to -120°C at which point the measurements were initiated unless otherwise stated.

Resulting spectra were processed and analysed using CasaXPS v2.3.19PR1.0. Peaks were fit with a Shirley background prior to component analysis. Components were fit using LA(1.3,253) lineshapes to obtain peak positions and FWHM.

3. Results and Discussion

Given the requirement for UHV conditions ($< 10^{-9}$ Torr) for the undertaking of XPS measurements, cooling was required to overcome the vapour pressure of the molecule (3.75 Torr at 293 K), with a temperature of below -30°C needed according to the Clausius-Clapeyron equation. The system was taken to -120°C in order to be completely confident in the stabilisation of the molecule within the vacuum chamber and under X-ray illumination (given the potential for localised heating under X-ray irradiation). Initial CryoXPS measurements revealed the major photoemissions, binding energies and peak fwhm for Ti 2p, O 1s and C 1s (Fig. 2). Ti 2p reported a single chemical environment with a Ti 2p_{3/2} peak maxima at 458.5 eV, a doublet separation of 5.8 eV, a Ti 2p_{3/2}: Ti 2p_{1/2} area ratio of 2:1 and a Ti 2p_{1/2}: Ti 2p_{3/2} FWHM ratio of 2.05:1 due to Coster-Kronig induced broadening.

The survey determined only the presence of Ti, O and C and the quantification of this is reported in Table 1. The quantification was found to be in relative agreement to the theoretical atomic ratios of the model compound. The carbon 1s region may be resolved by peak fitting into two components; the C-O alkoxide linkage (27%) and the CC/CH

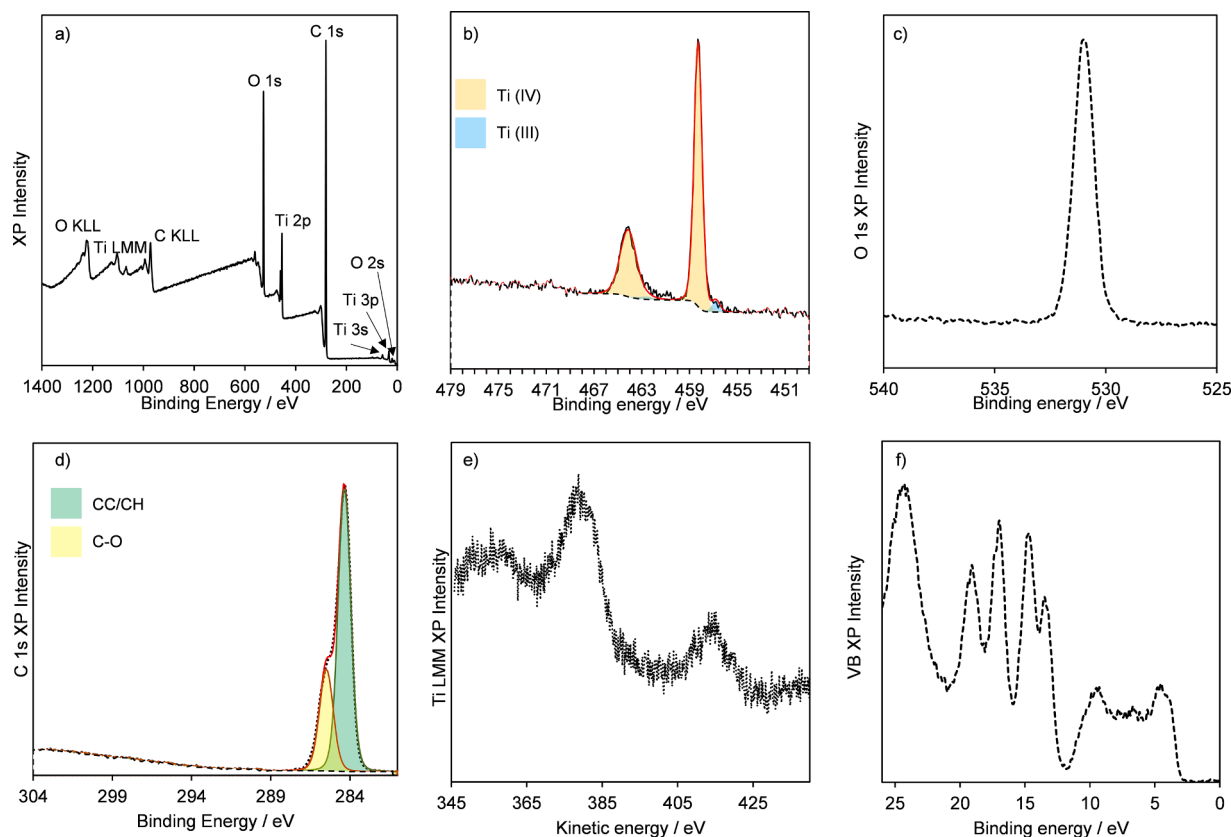


Fig. 2. (a) Survey, (b) Ti 2p, (c) O 1s, (d) Ti LMM, (e) C 1s and (f) Valence XPS spectra of titanium butoxide at -120°C

Table 1
Theoretical and measured atomic percentages of TBu.

Element	Theoretical At. %	Measured At. %
Ti	4.76	4.42
O	19.05	18.91
C	76.19	76.67

backbone (73%), which quantify at the expected ratio for the molecular structure.

The VB may be compartmentalised into 3 regions: 0-12 eV, comprising of the Ti d-band, C-C σ orbitals and O 2p band, [23] 12-21 eV, comprising of the ligand molecular orbitals, and 21-25 eV, comprising the O 2s peak. Of the central region, the peak at 13.3 eV may correspond to that of CH₃ π - and 14.5 eV to C-O σ -orbitals, [23] while the twin higher energy (17 & 19 eV) peaks have been ascribed to C 2s orbitals from the extended butyl chain. [24,25]

The peak properties are listed below in Tables 2 and 3.

Following a series of measurements it was observed that the Ti 2p region was indicating the presence of a small population of Ti³⁺ states, while the sample appeared to have degraded in colour (figure S1). A series of measurements were therefore recorded in order to determine the influence of X-ray exposure on these soft systems (Fig. 3). X-ray induced reduction occurred rapidly, with a recognisable Ti³⁺ feature appearing after minutes under the X-ray beam. For this reason, it is imperative that the analysis of the Ti 2p region be performed on a fresh spot and prior to any additional measurements. Furthermore, to prevent unwanted reduction, analysis spot optimisation ought to be performed on a separate region to the analysis area if using 'beam on' instrument auto-z functions, or aligned using optical methods providing optical cameras and microscopes are in good alignment with the analysis spot.

A very faint signal attributed to Ti³⁺ could be identified following a single acquisition under standard conditions (Fig. 4) by locking peak fitting parameters (peak position, fwhm) from a heavily reduced sample and applying this model across the series – with the compound reporting 4% Ti³⁺ in the initial sweep. Following prolonged exposure the degree of reduction reached a plateau at around 12% Ti³⁺ and remained stable for up to 1 hour under the illuminating beam.

The O 1s region was also monitored, to identify changes induced by reduction, though no significant peak intensity was identified from a secondary feature. The FWHM of the O 1s peak was found to broaden very slightly, although the overall peak position remained essentially unchanged (figure S2). This was attributed to the appearance of an O-Ti³⁺ bond, though deconvolution of the O 1s peaks was deemed unlikely to produce an accurate quantification of the sample given the apparent close proximity of the Ti-O-R and O-Ti³⁺ features.

In order to further investigate the relationship between analysis conditions and induced chemical changes to the sample, the analysis was repeated at a higher temperature of -60°C in order to increase the degree of reduction (figure S3) and more readily observe differences due to experimental parameter settings. At this higher temperature, we see an exaggerated reduction of the Ti(IV) towards Ti(III) and may observe more clearly the changing molecular chemistry. Analysis of the surface at varying X-ray powers revealed a clear trend in the rate of reduction as a function of illuminating flux (Fig. 5a). Furthermore, the effect of using the built in automatic sample height optimisation was monitored via analysis of a single scan following automatic and manual

Table 2
Photoelectron peak properties of titanium butoxide.

Photoelectron peak	Binding energy / eV	FWHM / eV
Ti 2p 3/2	458.5	0.8
Ti 2p 1/2	464.3	1.7
O 1s	531.0	1.1
C 1s (CC/CH)	284.8	0.9
C 1s (CO)	285.9	1.3

Table 3
Auger peak properties of titanium butoxide.

Auger peak	Kinetic energy / eV
Ti L ₃ M _{2,3} M _{4,5}	413.7
Ti L ₃ M _{2,3} M _{2,3}	378.4
O KLL	976.0
C KLL	259.3

height adjustment (figure S5). Automatic height adjustment, being a 'beam-on' technique, was found to reduce the molecule 5x more than by using the internal microscope to manually obtain the focal point prior to analysis.

In order to determine the origin of this reduction, be it primarily X-ray or electron (charge neutraliser) induced, a series of spectra were recorded with the flood gun both on and off. For the flood gun off experiment, one spectra was recorded with the charge neutraliser on, followed by 8 with the neutraliser off, followed by one final scan with the flood gun back on. This was compared to the start and end points of a series of 10 scans with the flood gun on for all 10 and degree of reduction calculated. The behaviour of the molecule under both conditions was essentially identical and led to the conclusion that this reduction was primarily X-ray induced. A similar process has been observed for Ti (IV) oxide clusters, in which excited photoelectrons have been shown to produce Ti³⁺ sites during X-ray irradiation. [26] Titanium (IV) alkoxides exist as tetramers with octahedral symmetry [27,28] consisting of both bridging and terminal alkoxide chains. During irradiation at -60°C, we do not see a change in the O:Ti ratio (figure S5), which suggests the molecules are not losing alkoxide ligands during this process. At these elevated temperature, we do now clearly see a broadening of the O 1s feature and high energy shoulder, potentially the formation of an O-Ti³⁺ site.

This molecule serves not only as a reference material for the materials scientist, but the resulting spectra highlight the importance of experimental consideration when undertaking measurements of this type. Low temperature XPS has the capability to provide essential insights into a wider range of fields than it currently typically does – particularly in the fields such catalysis (studying adsorbates) or environmental science (pollutants etc) in which understanding of solid-solution interfaces may be fundamental to developing new technologies.

Given a material demonstrating sensitivity to X-ray exposure, it is advised that the experimentalist ought ensure all care is taken in the experimental construction when analysing such materials by CryoXPS. A stepwise roadmap to analysis is outlined below.

1 Visually identify changes to the sample under X-ray exposure

Particularly important for materials whereby the vapour pressure at cryo temperatures is near to the critical limit under UHV conditions. The use of X-rays to irradiate a sample induces heating and, as such, may cause sublimation or melting when under the X-ray beam. Use internal cameras to monitor changes to the material appearance (colour/shape etc) with the beam on.

2 Chemically identify changes to the sample under X-ray exposure

Record data as individual scans, to be combined in post-analysis processing. This ensures that any changes to the chemistry at the surface may be readily identified by use of spectral overlays. Record each element at a fresh analysis area to observe potential changes on a shorter timescale.

3 Use non 'beam-on' sample height optimisation techniques.

Use of a well aligned optical camera will ensure any sample positioning procedures do not influence the surface chemistry or material

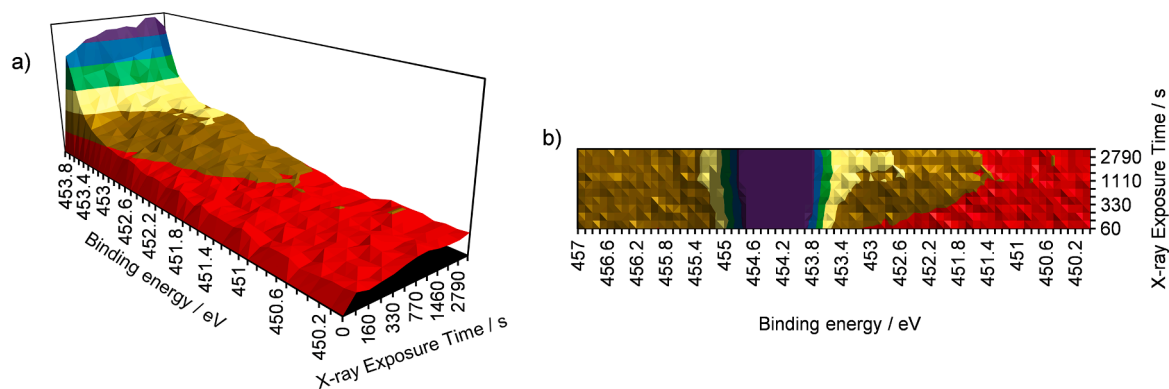


Fig. 3. (a) Visualisation of appearance of Ti 3+ feature following X-ray exposure and (b) full scan region of Ti 2p peak during X-ray exposure

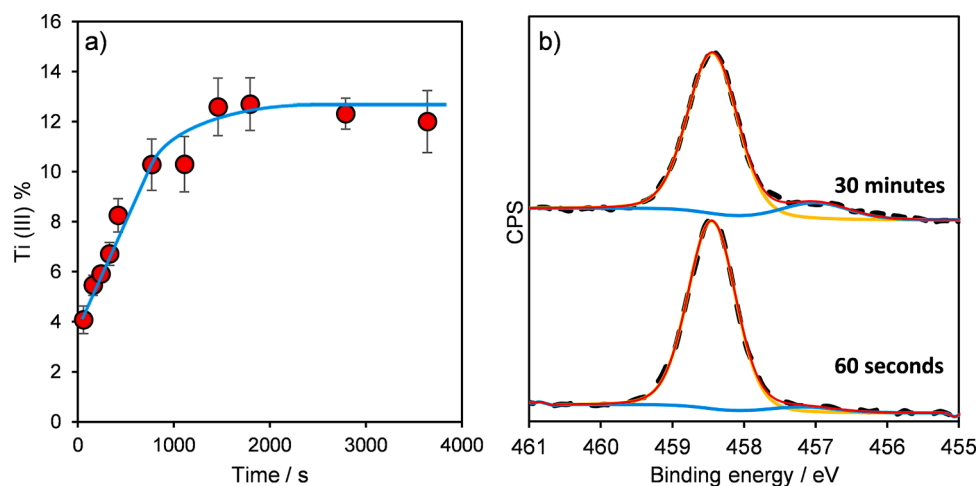


Fig. 4. (a) Quantification of Ti reduction degree as a function of X-ray exposure time and (b) representative XP spectra of Ti 2p for titanium butoxide at -120°C on a fresh sample and after 30 minutes exposure.

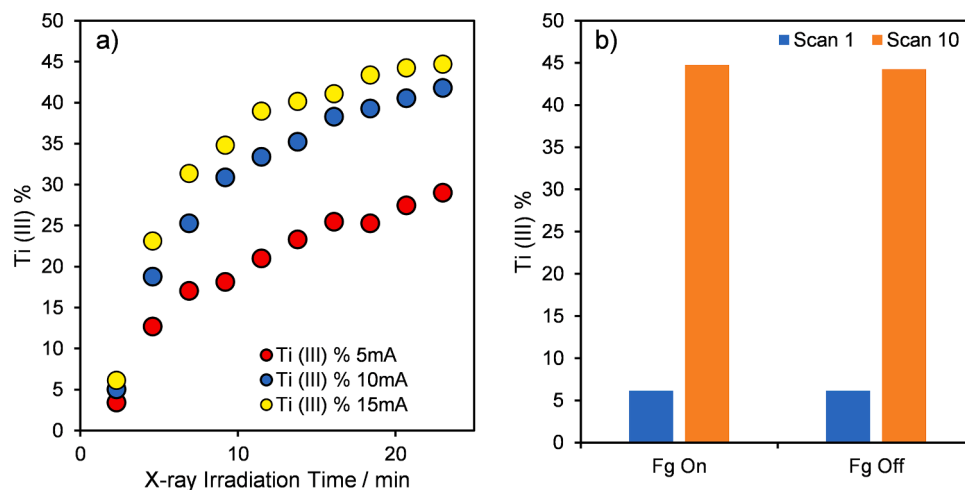


Fig. 5. (a) Degree of reduction using 5, 10 and 15 mA emission currents at -60°C and (b) degree of reduction following X-ray exposure with electron flood gun on vs off.

properties prior to XPS analysis.

4 Optimise analysis parameters to minimise damage

In systems such as the aforementioned, where photoelectronic

emission intensity is strong for each region of interest, consider lowering the X-ray emission current and/or increasing the analyser pass energy (thus reduced required time for analysis) in order to reduce the heat transfer from irradiation/photo-induced chemical damage to the sample surface.

5 Analyse multiple areas

If signal-to-noise a concern, record single scans on multiple analysis areas and combine during post-analysis. This will enable longer analysis times without sacrificing sample condition. Consider this as a potential requirement when preparing the sample, and ensure a large enough area has been loaded for the eventuality that multiple analysis spots are needed. One must also consider the total X-ray illumination area for this step (separate to the 'analysis area' in the case of selected area analysis using electromagnetic lens modes rather than microfocused X-ray beams), in order to avoid analysing areas previously exposed to X-rays even if they were not part of the analysis area.

4. Conclusions

Photoelectron spectra analysis of titanium butoxide was obtained via *in-situ* cooling in order to stabilise the compound under vacuum. It was observed both visually and spectroscopically that this compound underwent rapid reduction when under X-ray illumination within a UHV chamber. A number of experimental protocols were employed in order to secure a reliable set of spectra for these materials, including avoiding using an X-ray trace to align the sample height and analysis position and recording multiple analysis areas across the sample to avoid recording degraded spectra.

Declaration of Competing Interest

The authors declare that they have no known competing financial interests or personal relationships that could have appeared to influence the work reported in this paper.

Data availability

Data will be made available on request.

Acknowledgements

The X-ray photoelectron (XPS) data collection was performed at the EPSRC National Facility for XPS ("HarwellXPS"), operated by Cardiff University and UCL, under Contract No. PR16195. I wholeheartedly thank the reviewers for their valuable time in providing a constructive and high quality reviewing process.

Supplementary materials

Supplementary material associated with this article can be found, in the online version, at [doi:10.1016/j.apsadv.2023.100467](https://doi.org/10.1016/j.apsadv.2023.100467).

References

- [1] R. Trofimovaite, C.M.A. Parlett, S. Kumar, L. Frattini, M.A. Isaacs, K. Wilson, L. Olivi, B. Coulson, J. Debgupta, R.E. Douthwaite, A.F. Lee, Single atom Cu(I) promoted mesoporous titania for photocatalytic Methyl Orange depollution and H₂ production, *Applied Catalysis B: Environmental* 232 (2018) 501–511.
- [2] V. Hiremath, V.G. Deonikar, H. Kim, J.G. Seo, Hierarchically assembled porous TiO₂ nanoparticles with enhanced photocatalytic activity towards Rhodamine-B degradation, *Colloids and Surfaces A: Physicochemical and Engineering Aspects* 586 (2020), 124199.
- [3] H. Kominami, J.-i. Kato, Y. Takada, Y. Doushi, B. Ohtani, S.-i. Nishimoto, M. Inoue, T. Inui, Y. Kera, Novel synthesis of microcrystalline titanium (IV) oxide having high thermal stability and ultra-high photocatalytic activity: thermal decomposition of titanium (IV) alkoxide in organic solvents, *Catalysis Letters* 46 (1997) 235–240.
- [4] G. Man, J. Schwartz, J.C. Sturm, A. Kahn, Electronically Passivated Hole-Blocking Titanium Dioxide/Silicon Heterojunction for Hybrid Silicon Photovoltaics, *Advanced Materials Interfaces* 3 (2016), 1600026.
- [5] G. Sahasrabudhe, Low Temperature Solution-Based Treatment for Highly Passivated Si/TiO₂ Heterojunction, in: *International Conference on Advances in Thermal Systems, Materials and Design Engineering (ATSMDE2017)*, 2017.
- [6] M.A. Isaacs, B. Barbero, L.J. Durndell, A.C. Hilton, L. Olivi, C.M.A. Parlett, K. Wilson, A.F. Lee, Tunable Silver-Functionalized Porous Frameworks for Antibacterial Applications, *Antibiotics* 7 (2018) 55.
- [7] M.H.A. Rehim, M.A. El-Samahy, A.A. Badawy, M.E. Mohram, Photocatalytic activity and antimicrobial properties of paper sheets modified with TiO₂/Sodium alginate nanocomposites, *Carbohydrate polymers* 148 (2016) 194–199.
- [8] M.A. Isaacs, C.M. Parlett, N. Robinson, L.J. Durndell, J.C. Manayil, S.K. Beaumont, S. Jiang, N.S. Hondow, A.C. Lamb, D. Jampaiah, A spatially orthogonal hierarchically porous acid–base catalyst for cascade and antagonistic reactions, *Nature Catalysis* 3 (2020) 921–931.
- [9] F. Bérubé, B. Nohair, F. Kleitz, S. Kaliaguine, Controlled Postgrafting of Titanium Chelates for Improved Synthesis of Ti-SBA-15 Epoxidation Catalysts, *Chemistry of Materials* 22 (2010) 1988–2000.
- [10] M. Landau, L. Vradman, X. Wang, L. Titelman, High loading TiO₂ and ZrO₂ nanocrystals ensembles inside the mesopores of SBA-15: preparation, texture and stability, *Microporous and mesoporous materials* 78 (2005) 117–129.
- [11] C.M. Parlett, L.J. Durndell, A. Machado, G. Cibin, D.W. Bruce, N.S. Hondow, K. Wilson, A.F. Lee, Alumina-grafted SBA-15 as a high performance support for Pd-catalysed cinnamyl alcohol selective oxidation, *Catalysis Today* 229 (2014) 46–55.
- [12] M. Ramstedt, L. Leone, P. Persson, A. Shchukarev, Cell wall composition of *Bacillus subtilis* changes as a function of pH and Zn²⁺ exposure: insights from cryo-XPS measurements, *Langmuir* 30 (2014) 4367–4374.
- [13] A. Cano, L. Lartundo-Rojas, A. Shchukarev, E. Reguera, Contribution to the coordination chemistry of transition metal nitroprussides: a cryo-XPS study, *New Journal of Chemistry* 43 (2019) 4835–4848.
- [14] A. Shchukarev, M. Ramstedt, Cryo-XPS: probing intact interfaces in nature and life, *Surface and Interface Analysis* 49 (2017) 349–356.
- [15] M. Kjærviik, M. Ramstedt, K. Schwibbert, P.M. Dietrich, W.E. Unger, Comparative study of NAP-XPS and cryo-XPS for the investigation of surface chemistry of the bacterial cell-envelope, *Frontiers in Chemistry* 9 (2021), 666161.
- [16] A. Shchukarev, Z. Gojkovic, C. Funk, M. Ramstedt, Cryo-XPS analysis reveals surface composition of microalgae, *Applied Surface Science* 526 (2020), 146538.
- [17] Y. Huai, Y. Qian, Y. Peng, Re-evaluating the sulphidisation reaction on malachite surface through electrochemical and cryo XPS studies, *Applied Surface Science* 531 (2020), 147334.
- [18] S. Jelavić, N. Bovet, S.L. Stipp, Cryogenic X-ray photoelectron spectroscopy (cryo-XPS) study of natural and synthetic kaolinites in MgCl₂ solutions, in: *Clays, Clay Minerals and Layered Materials-CMLM2013* (2013) 120. -120.
- [19] M. Ejtemaei, A.V. Nguyen, Characterisation of sphalerite and pyrite surfaces activated by copper sulphate, *Minerals engineering* 100 (2017) 223–232.
- [20] M.F. Delcroix, E.M. Zuyderhoff, M.J. Genet, C.C. Dupont-Gillain, Optimization of cryo-XPS analyses for the study of thin films of a block copolymer (PS-PEO), *Surface and Interface Analysis* 44 (2012) 175–184.
- [21] Z. Zhao, Z. Yuan, X. Zhang, F. Liu, Design of a Cryogenic Air-Free Sample Transfer System to Enable Volatile Materials Analysis with X-ray Photoelectron Spectroscopy, *Chemistry of Materials* 33 (2021) 9101–9107.
- [22] Y. Mikhlin, A. Romanchenko, Y. Tomashevich, Surface and interface analysis of iron sulfides in aqueous media using X-ray photoelectron spectroscopy of fast-frozen dispersions, *Applied Surface Science* 549 (2021), 149261.
- [23] M. Faubel, B. Steiner, J.P. Toennies, Photoelectron spectroscopy of liquid water, some alcohols, and pure nonane in free micro jets, *The Journal of chemical physics* 106 (1997) 9013–9031.
- [24] J.-J. Pireaux, S. Svensson, E. Basilier, P.-Å. Malmqvist, U. Gelius, R. Caudano, K. Siegbahn, Core-electron relaxation energies and valence-band formation of linear alkanes studied in the gas phase by means of electron spectroscopy, *Physical Review A* 14 (1976) 2133.
- [25] J.-J. Pireaux, R. Caudano, X-ray photoemission study of core-electron relaxation energies and valence-band formation of the linear alkanes. II. Solid-phase measurements, *Physical Review B* 15 (1977) 2242.
- [26] T. Bennett, R.H. Adnan, J.F. Alvino, R. Kler, V.B. Golovko, G.F. Metha, G. G. Andersson, Effect of Gold Nanoclusters on the Production of Ti³⁺ Defect Sites in Titanium Dioxide Nanoparticles under Ultraviolet and Soft X-ray Radiation, *The Journal of Physical Chemistry C* 119 (2015) 11171–11177.
- [27] S. Weymann-Schildknecht, M. Henry, Mechanistic aspects of the hydrolysis and condensation of titanium alkoxides complexed by tripodal ligands, *Journal of the Chemical Society, Dalton Transactions* (2001) 2425–2428.
- [28] D. Bradley, C. Holloway, Nuclear magnetic resonance and cryoscopic studies on some alkoxides of titanium, zirconium, and hafnium, *Journal of the Chemical Society A: Inorganic, Physical, Theoretical* (1968) 1316–1319.